JCTC Journal of Chemical Theory and Computation

Article

pubs.acs.org/JCTC

Balancing Exchange Mixing in Density-Functional Approximations for Iron Porphyrin

Victoria E. J. Berryman, Russell J. Boyd, and Erin R. Johnson*

Department of Chemistry, Dalhousie University, 6274 Coburg Road, Halifax, Nova Scotia Canada, B3H 4R2

Supporting Information

ABSTRACT: Predicting the correct ground-state multiplicity for iron(II) porphyrin, a high-spin quintet, remains a significant challenge for electronic-structure methods, including commonly employed density functionals. An even greater challenge for these methods is correctly predicting favorable binding of O_2 to iron(II) porphyrin, due to the open-shell singlet character of the adduct. In this work, the performance of a modest set of contemporary density-functional approximations is assessed and the results interpreted using Bader delocalization indices. It is found that inclusion of greater proportions of Hartree−Fock exchange, in hybrid or range-separated hybrid functionals, has opposing effects; it improves the ability of the functional to identify the ground state but is detrimental to predicting favorable dioxygen binding. Because of the uncomplementary nature of these properties, accurate prediction of both the relative spin-state energies and the O_2 binding enthalpy eludes conventional density-functional approximations.

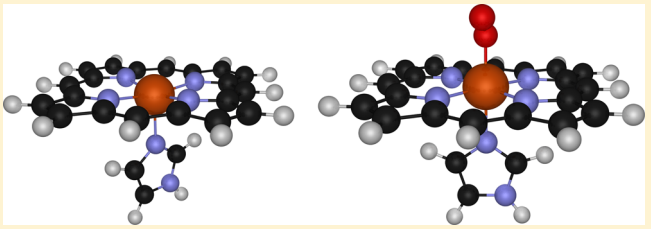

1. INTRODUCTION

Porphyrins are a prominent class of molecules found ubiquitously in nature, most notably as the red pigment of blood and the green pigment of leaves. Many biological proteins have active sites that feature metalloporphyrin centers. These systems represent a significant area of research due to their diverse chemical applicability and potential for diagnostic and therapeutic purposes.[1,2] Iron-centered systems in particular have attracted much interest due to the biological relevance of heme, known universally to occur in the oxygen-carrying proteins hemoglobin and myoglobin, as well as in enzymes such as cytochrome *c* and peroxidase.[3−5] The functionality of the hemoglobin protein is, in part, due to the high-spin state of the iron atom located in the iron-porpyhrin structure at the center of the heme group and that the spin state of the system changes upon dioxygen binding.

The simplest, unsubstituted porphyrin is known as a porphine, and iron porphine is frequently used as a model to study the chemistry of heme. Since this system is characterized by multiple spin states that are relatively close in energy, it presents a particular challenge to quantum-chemistry methods to predict accurately the correct ground state. Another challenging feature is the complex electronic structure of the oxy-iron porphine that results from dioxygen binding. This makes the ability to describe iron-porpyhrin chemistry an attractive test of contemporary density-functional methods.

Density-functional theory (DFT) is the most widely used electronic structure method for efficient calculations on chemical systems. However, despite its widespread popularity, there are important limitations of DFT methods that are apparent in some chemical systems. One such error is the many-electron self-interaction error, or delocalization error,[6−11] which is a common problem for popular density functionals, in particular generalized gradient approximations (GGAs).[12−18] This is because the assumption of a localized exchange-correlation hole leads to failures in the calculation of, for example, dissociation barriers and long-range charge-transfer excitations, due to artificial stabilization of delocalized states. Hybrid functionals attempt to reduce this error by including a constant portion of nonlocal Hartree−Fock (HF) exchange (usually 20−50%). Alternatively, range-separated hybrid functionals involve a variable mixing of local and nonlocal exchange, commonly approaching full HF exchange in the limit of long-range electron−electron interactions. The electron repulsion, $1/r_{12}$, is partitioned into short-range and long-range terms, where the range-separation parameter ω controls the length scale of this partitioning.[19−21,21−25]

$$\frac{1}{r_{12}} = \frac{\mathrm{erf}(\omega r_{12})}{r_{12}} + \frac{\mathrm{erfc}(\omega r_{12})}{r_{12}} \quad (1)$$

The first and second terms of eq 1 are the long-range and short-range portions of the electron repulsion, typically described by HF and GGA exchange, respectively. As ω increases, a greater proportion of the electronic interactions is treated by the long-range description. The erf and erfc functions, known as the error function and complementary error function, respectively, are used to ensure the terms sum to unity.

This study aims to investigate the performance of common density functionals for an iron-porphyrin model system, focusing on the prediction of the correct ground-state spin multiplicity and the dioxygen binding energy. The role of the

Received: March 2, 2015

DOI: 10.1021/acs.jctc.5b00203
J. Chem. Theory Comput. XXXX, XXX, XXX−XXX

exchange functional is highlighted, and the results are interpreted using delocalization indices obtained from the quantum theory of atoms in molecules (QTAIM). It is found that inclusion of short-range exact exchange is necessary to identify the correct ground-state of the iron porphine but precludes prediction of favorable dioxygen binding due to the multireference nature of the open-shell singlet state of the oxy-iron adduct.

2. COMPUTATIONAL METHODS

A model system comprised of an iron porphine (FeP) with an imidazole (Im) axial ligand, shown in Figure 1 and denoted as

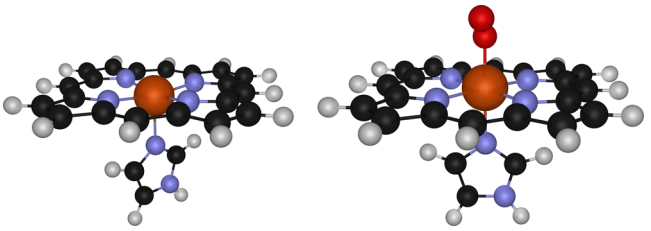

Figure 1. Model systems used in this study for FePIm (left) and FePIm-O_2 (right). Carbon atoms are represented in black, nitrogen in blue, oxygen in red, hydrogen in white, and iron in orange.

FePIm, is used to model the heme and histidine groups. This is a common model system employed to represent the active sites of both hemoglobin and myoglobin, since it retains the central feature of heme and has been used in previous computational studies.[26−33] A model system is essential since modeling the entire heme group with quantum-mechanical methods would not be computationally feasible. Dioxygen binding to the heme group is modeled by the FePIm system with dioxygen bound to the remaining axial coordination site of the iron, denoted FePIm-O_2, and also shown in Figure 1.

All density-functional calculations used the Gaussian 09 program package.[34] The spin-unrestricted formalism was employed throughout, due to the high-spin nature of the FePIm system and because the FePIm-O_2 system is known to be an open-shell singlet that resembles a low-spin Fe(III) center antiferromagnetically coupled to a superoxide radical anion.[35] Geometry optimizations and frequency calculations were performed for all species with the B97-D method.[36] Single-point energies were then calculated with other selected functionals at the optimized B97-D geometries. All energies reported herein are corrected for zero-point and thermal effects at the B97-D level and correspond to gas-phase enthalpies or Gibbs energies at 298 K.

In the first part of this study, 11 density-functional approximations (DFAs) were compared: the BLYP,[37,38] BLYP-D, and B97-D[36] GGAs; the B3LYP,[38,39] B3LYP-D, PBE0,[40,41] M06,[42] and M06-2X[42] hybrid functionals; and the ωB97,[24] ωB97X,[24] and ωB97X-D[25] range-separated hybrids. A number of these functionals include empirical dispersion corrections,[36] as indicated with the "-D" notation. Including dispersion interactions improves calculated binding energies for a variety of transition metal complexes.[31,43]

Two basis set schemes were employed, both composed of Pople-type basis sets. The first employs locally dense basis sets[44] for computational efficiency and allows for a high level calculation on the central region of the system, where the binding interactions occur. This basis set, denoted basis set I, employs 6-311+G* on iron, nitrogen, and oxygen, and 6-31G on carbon and hydrogen. This approach has been shown to be successful for heme systems.[45] The second basis set, denoted basis set II, employs 6-311+G(2df,p) for all atoms. This larger basis set is suitable for single-point calculations, but optimizations are not computationally efficient for exploration of the potential-energy surface. Nevertheless, we note that the effect of basis-set size is small. With BLYP, the computed differences between basis sets I and II for the relative spin-state energies and oxygen binding enthalpies are 0.5 and 1.3 kcal/mol, respectively.

The second part of this study investigates the effects of including HF exchange and long-range corrections on the spin-state energetics and dioxygen binding enthalpy of the iron porphine system. Single-point calculations with BLYP-based hybrid functionals were performed, using basis set I and the previously optimized structures, with the amount of HF exchange systematically varied. Similarly, the characteristic length scale of the range-separation, defined by ω, was also systematically varied in a series of LC-BLYP calculations.

Finally, the quantum theory of atoms in molecules, QTAIM,[46] was employed to study the chemical bonding in the iron-porphine complexes. QTAIM involves the analysis of the topology of the one-electron density; however, two-electron properties, based on the electron pair density, can also provide insight into chemical properties. The electron pair density, denoted $\rho(\mathbf{r}_1,\mathbf{r}_2)$, represents the probability of simultaneously finding an electron at points $\mathbf{r}_1$ and $\mathbf{r}_2$ and contains information about electron correlation. A two-electron property employed for analysis in this work is the delocalization index,[47−50] denoted as δ. If atomic basins A and B are considered, the delocalization index provides a quantitative measure of the bond order or sharing of electrons between atoms A and B and is obtained by integrating the pair density over the atomic basins.

It should be noted that, since the electron-pair density is not defined within density-functional theory, what is measured is the delocalization of the exact exchange hole constructed from the Kohn−Sham orbitals. It has been shown that the delocalization indices obtained via the Kohn−Sham orbitals slightly overestimate delocalization, or covalency, relative to those computed from the HF orbitals.[51,52] Although not theoretically rigorous, the delocalization indices derived from DFT methods have been shown to be quite useful tools for analysis of molecular electronic structure.[49,50,53,54] In this work, QTAIM atomic charges and delocalization indices were computed using the AIMAll software.[55]

3. RESULTS AND DISCUSSION

3.1. The Iron Porphine Model System. The FePIm model system was first optimized in both the triplet and quintet spin states. Only these states were considered, as the singlet state has been consistently shown to be much higher in energy than the intermediate and high-spin states.[26,30,32,33,56] Human deoxy-hemoglobin exists in the quintet state;[56] however, it is common for density-functional approximations to favor lower spin multiplicities, thus incorrectly determining the ground state. This is a well-known error when a given electron configuration has multiple spin states that are close in energy, which is especially common in transition metal complexes.[57−59] Thus, the energetics of the spin states are sensitive to the details of the exchange-correlation functional, and it is important to

DOI: 10.1021/acs.jctc.5b00203
J. Chem. Theory Comput. XXXX, XXX, XXX−XXX

consider functional performance with respect to the relative spin-state energies.

Geometrical parameters for the triplet and quintet states of FePIm are reported in Table 1, where N_{Im} indicates the imidazole nitrogen and Fe−N_p the porphyrin nitrogen. Doming refers to the displacement of the Fe atom from the plane of the porphyrin ring. Experimental data, based on crystallographic studies for the deoxy forms of myglobin and hemoglobin predict a Fe−N_{Im} distance of 2.06−2.15 Å, a Fe−N_p distance of 2.036−2.124 Å, and an Fe out-of-plane displacement (doming) of 0.290−0.365 Å.[60−62] These values are in agreement with the results in Table 1 for the quintet state. Although the doming is slightly underestimated by the B97D functional, the results are impressive considering the lack of the protein environment in the computational model. Of importance is the correct increase in doming observed from the low-spin state to the high-spin state. For comparison, in a previous study, the B3LYP functional predicted doming of 0.14 and 0.36 Å for the triplet and quintet states, respectively.[27]

Table 1. Geometrical Parameters (Distances in Å and Angles in deg) for the Triplet (S = 1) and Quintet (S = 2) States of FePIm and for the Open-Shell Singlet State of FePIm-O_2 (S = 0)

	FePIm		FePIm-O_2
quantity	S = 1	S = 2	S = 0
Distances (Å)			
Fe−N_{Im}	2.162	2.128	2.077
Fe−N_p	2.014	2.082	2.021
Fe−O			1.846
O−O			1.275
doming	0.080	0.282	0.053
Angles (deg)			
Fe−O−O			121.0

The geometrical parameters for the oxy-iron porphine model system are also shown in Table 1. Upon dioxygen binding, both types of Fe−N bonds shorten, indicating a contracted system in the bound state. The results are in excellent agreement with experiments for oxymyoglobin, which report a Fe−N_{Im} distance of 2.06−2.08 Å, O−O distance of 1.24−1.25 Å, and Fe−O−O angle of 122−124°.[61,63]

It is well-known that oxyhemoglobin is diamagnetic, having an open-shell singlet state.[64] The spin populations, based on QTAIM analysis, are predicted to be 0.992 au on the iron atom, and −0.367 au and −0.578 au on the proximal and distal oxygen atoms, respectively. A spin-density difference plot is shown in Figure 2 and the open-shell singlet nature of the complex is evident from the localization of a significant portion of the α-spin density on the dioxygen ligand and β-spin density on the iron. There is also a small amount of spin density delocalized over the porphine ring and the coordinating N atom of the imidazole ligand. In addition to the spin density difference plot, the highest singly-occupied molecular orbitals (SOMO) of both α- and β-spin are also shown in Figure 2. These show the localization of the α-SOMO on the dioxygen, resembling the σ^* orbital of O_2, and the β-SOMO on the iron and porphine ring, resembling the d_{xz} iron atomic orbital. These molecular orbitals form the dominant contributions to the spin-density difference plot.

3.2. Comparison of Functionals. The Gibbs energy difference between the triplet and quintet states of FePIm, denoted here by ΔG_S, is defined as

$$\Delta G_S = G_{triplet} - G_{quintet} \quad (2)$$

Thus, a functional that produces a positive value for ΔG_S correctly predicts the quintet ground state for the system. The Fe−O bond dissociation enthalpy, abbreviated as ΔH_B, is defined as the enthalpy difference between the infinitely separated reactants (the quintet state of FePIm and the triplet state of O_2) and the bound system, FePIm-O_2:

$$\Delta H_B = (H_{\mathrm{FePIm}} + H_{\mathrm{O_2}}) - H_{\mathrm{FePIm\text{-}O_2}} \quad (3)$$

Thus, a positive ΔH_B indicates favorable O_2 binding, and a negative value indicates unfavorable O_2 binding.

Table 2 reports the results for ΔG_S and ΔH_B with all of the DFAs investigated in this study. The data shows that only the B97-D, B3LYP-D, and ωB97X-D functionals are capable of producing both the correct ground state and favorable O_2 binding; further, only B97-D approaches the experimental ΔH_B value of 12.6 kcal/mol. While the relative energy of the triplet and quintet states of FePIm (termed the intermediate- and high-spin states, respectively) is not known experimentally, it has been established that the high-spin state is the ground state. Theoretical predictions using CASPT2, a multireference

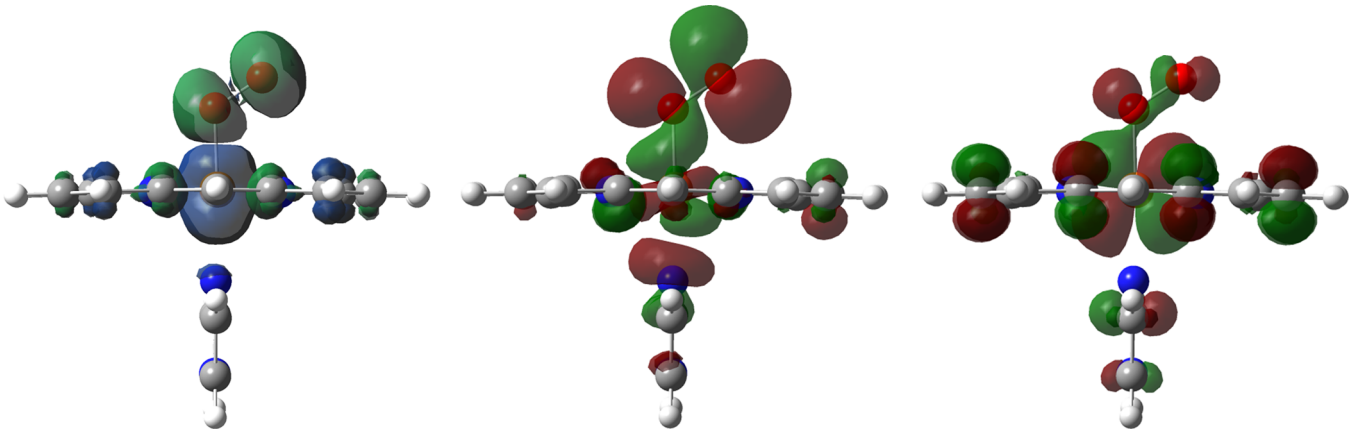

Figure 2. Spin-density difference plot for FePIm-O_2 (left), with an isosurface of 0.001 au. The green surface corresponds to an excess of α-electron density, and the blue surface corresponds to an excess of β-electron density. Also shown are the α-spin (center) and β-spin (right) singly occupied molecular orbitals (SOMO) for FePIm-O_2, with an isosurface of 0.02 au.

DOI: 10.1021/acs.jctc.5b00203
J. Chem. Theory Comput. XXXX, XXX, XXX−XXX

Table 2. Comparison of the Relative Spin-State Energies, ΔG_S, and the Fe−O Bond Dissociation Ethalpies, ΔH_B, in kcal/mol[a]

functional	%HF	ΔG_S	ΔH_B
B97-D	0	0.8	11.7
BLYP	0	−9.6	24.0
BLYP-D	0	−11.4	34.5
B3LYP	20	1.8	−1.0
B3LYP-D	20	0.3	8.2
PBE0	25	3.8	−4.3
M06	27	3.3	−2.5
M06-2X	54	15.8	−27.4
ωB97	0 (0.4)	−1.1	0.0
ωB97X	16 (0.3)	0.5	−1.9
ωB97X-D	22 (0.2)	10.3	3.5
expt		>0	12.6

[a]All values were computed using basis set II: 6-311+G(2df,p). ΔH_B is expressed relative to the high-spin state of FePIm. For each functional, the fraction of HF exchange is given; for the range-separated, the value corresponds to the percentage of short-range exact exchange and the ω value (in au^{-1}) is in parentheses. Experimental values are also reported.[65]

method, estimate the energy difference between these spin states to be approximately 10 kcal/mol,[32,33] indicating that B97-D and B3LYP-D do not sufficiently stabilize the quintet state and only ωB97X-D gives an accurate prediction of ΔG_S. In general, Hartree−Fock calculations overstabilize high-spin states and GGA functionals overstabilize low-spin states.[57]

From Table 2, the BLYP, BLYP-D, and ωB97 functionals all predict the triplet state to be most stable, which implies that inclusion of some short-range HF exchange is critical to obtain the correct ground state. On the other hand, for the majority of the hybrid functionals listed in Table 2, the Fe−O bond enthalpy is erroneously predicted to be negative,or non-bonding. Notably, the M06-2X functional predicts the greatest nonbonding character and includes the highest amount of exact exchange of the functionals considered.

The effect of dispersion on the dioxygen binding enthalpy can be seen by comparing BLYP, B3LYP, and ωB97X, with the analogous dispersion corrected DFAs: BLYP-D, B3LYP-D, and ωB97X-D, respectively. In all cases, the DFAs predict increased binding when dispersion is included, in agreement with previous findings.[31] This is not surprising since including dispersion accounts for additional stabilizing interactions between the oxygen atoms and the FePIm complex, which are important for predicting accurate bond-dissociation enthalpies.[66] The effects are most clearly shown for the BLYP and B3LYP DFAs and their dispersion corrected analogues, where the dispersion contribution is ca. 10 kcal/mol. Comparing ωB97X with ωB97X-D involves varied exchange parameters in addition to the dispersion correction.

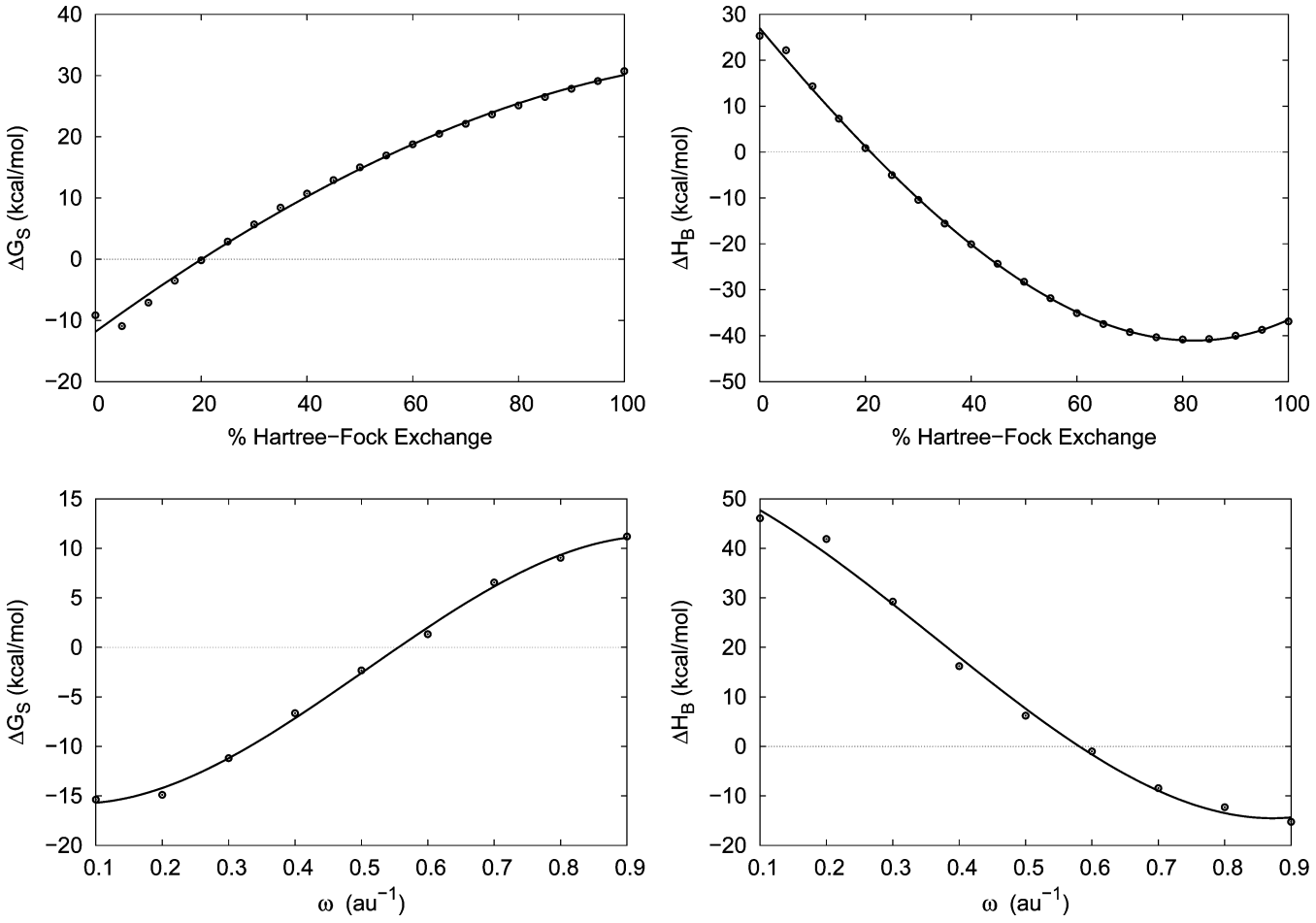

Figure 3. Effect of the percentage of HF exchange (top) and the range-separation parameter, ω (bottom), on the relative energy difference, ΔG_S, between the quintet and triplet spin states of FePIm (left) and on the FePIm-O_2 bond dissociation enthalpy, ΔH_B (right), in kcal/mol.

DOI: 10.1021/acs.jctc.5b00203
J. Chem. Theory Comput. XXXX, XXX, XXX−XXX

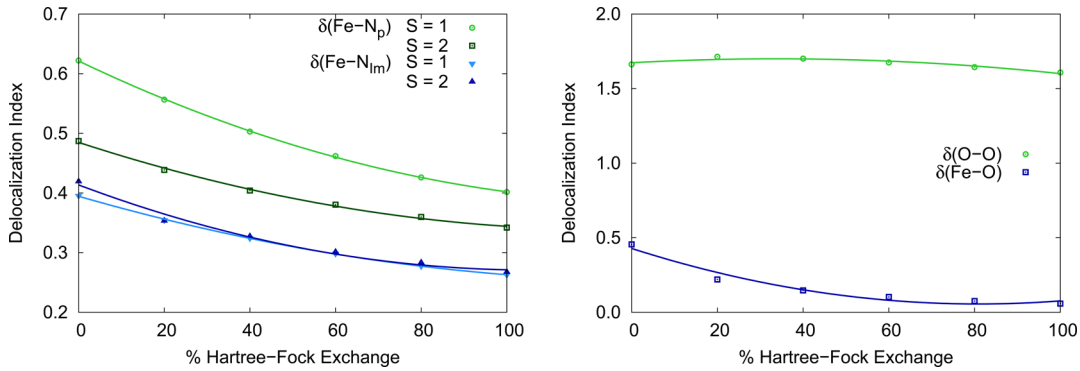

Figure 4. Delocalization index, δ, for the Fe−N_{Im} and Fe−N_P bonds in the triplet and quintet states of FePIm (left), and for the O−O and Fe−O bonds in FePIm-O_2 (right), with respect to varied HF exchange.

It is also interesting to consider the range-separated DFAs: ωB97, ωB97X, and ωB97X-D, each of which enacts 100% HF exchange for long-range electron−electron interactions but with differing short-range contributions and ω values (see Table 2). With only long-range HF exchange, as in ωB97, the correct ground state is not predicted; however, unfavorable binding is predicted, nonetheless. This suggests that the Fe−O bond-dissociation enthalpy is more sensitive to the addition of long-range HF exchange than is the relative spin-state energy. For the ωB97X and ωB97X-D functionals, the correct high-spin ground state is determined. The ωB97X-D functional predicts a significantly higher value of ΔG_S, or greater stability for the high-spin state, relative to the intermediate-spin state. Thus, accurate prediction of ΔG_S requires the addition of short-range HF exchange. Finally, only ωB97X-D predicts favorable dioxygen binding, which is likely a result of both the inclusion of a dispersion correction and the effect of a decreased ω.

3.3. Effect of Exchange on Spin States. As discussed above, predicting the correct ground state is not a trivial task for density-functional approximations. The effect of varying either the percentage of Hartree−Fock exchange included in the functional or the range-separation parameter, ω, on ΔG_S is investigated in detail, and the results are shown in Figure 3. The correct high-spin ground state is predicted when the functional contains greater than 20% HF exchange, or when ω is greater than ca. 0.56 au^{-1}. This is a relatively large ω value, or a short interelectronic distance, with respect to popular long-range corrected functionals,[24,25,67] again suggesting that fairly short-range exact exchange is important for the correct ordering of spin states.

In the HF description of multiple spin states, the energy difference between any two states with the same electron configuration is given by the exchange integral. Since they differ only in electron spin, these states yield similar electron densities. Because the exchange-correlation functional depends only on local properties of the electron density, the resulting energy difference becomes difficult to determine with DFT and is strongly dependent on the features of the chosen functional.[57−59]

The effect of exact exchange on the chemical bonding in the triplet and quintet states of the FePIm complex is illustrated in Figure 4, which plots the delocalization index for both the Fe−N_{Im} and Fe−N_P bonds. In all cases, the delocalization index decreases as the amount of HF exchange is increased, indicating that adding HF exchange results in decreased electron density in the π-conjugated system of the porphyrin ring and, consequently, increased localization of electron density near the atomic centers. This is expected given the tendency of GGAs to favor greater electron delocalization and HF to favor electron localization.[10,11,22,68] Also, δ(Fe−N_{Im}) is found to be effectively independent of the spin state, while δ(Fe−N_P) is significantly higher in the triplet state, relative to the quintet, for all exchange mixing fractions. This indicates that the triplet has greater electron delocalization and stronger Fe−N_P bonds, in agreement with the shorter bond lengths in Table 1. This is consistent with previous work,[27] which argued that weakening of the Fe−N_P bonds in the quintet, due to the high-spin orbital occupation, is responsible for its increased doming (see Table 1). Furthermore, this is also consistent with the predicted spin-state energies, where GGA functionals favor the more delocalized triplet state and the functionals with the highest fractions of exact exchange favor the more localized quintet state (Table 2).

3.4. Effect of Exchange on Binding Enthalpy. As noted above, modeling oxygen binding to the iron-porphine system is a significant challenge for density-functional approximations, and all functionals that include Hartree−Fock exchange, such as conventional hybrids, predict unfavorable oxygen binding. To more clearly discern the effect of the exchange functional, the dependence of the Fe−O bond-dissociation enthalpy, ΔH_B, on the percentage of Hartree−Fock exchange or the range-separation parameter, ω, is shown in Figure 3. The results are effectively the opposite of those seen for the relative spin-state energies: binding is favorable only if the amount of HF exchange is less than ca. 20% or when ω is less than ca. 0.58 au^{-1}. Thus, including HF exchange in a hybrid or range-separated hybrid DFA is detrimental to predicting favored dioxygen binding.

The poor performance of functionals including some HF exchange for the FePIm-O_2 open-shell singlet results from the failure to capture static, or nondynamical, correlation.[69] Open-shell singlet states cannot be represented by a single Slater determinant, and multireference methods are needed to describe such strongly correlated systems.[70,71] Previous multireference analysis suggests that the wave function for the FePIm-O_2 system is comprised of a mixture of many configurations, including the Pauling, Weiss, and McClure configurations.[72] The Pauling configuration is a closed-shell interaction between singlet Fe(II) and singlet O_2, the Weiss configuration is the antiferromagnetically coupled interaction between doublet Fe(III) and doublet O_2^-, and the McClure configuration is the interaction between triplet Fe(II) and triplet O_2. HF and DFT methods are based on single determinants and thus cannot capture the complex, multi-

DOI: 10.1021/acs.jctc.5b00203
J. Chem. Theory Comput. XXXX, XXX, XXX−XXX

reference character of the FePIm-O_2 ground state. However, the tendency of GGAs to give a localized exchange-correlation hole, which leads to delocalization error, means that they are fortuitously able to include some effects of strong correlation[69] and provide a reasonable prediction of the binding in this case.

The variation of the Fe−O and O−O delocalization indices in the FePIm-O_2 complex with the LC-BLYP range-separation parameter is shown in Figure 4. More favorable binding results from greater electron delocalization across the Fe−O bond. As shorter-range exact exchange is included in the functional, δ(Fe−O) decreases from 0.46 to 0.06, illustrating the weakening of the Fe−O bond. Thus, the addition of HF exchange causes the Fe−O interaction to become nonbonding in character. However, δ(O−O) remains effectively constant at 1.6, and thus the O−O bond is similar to that of superoxide, which has a formal bond order of 1.5.

The QTAIM atomic charges also vary with inclusion of exact exchange, and the results are summarized with respect to the Fe−O bond-dissociation enthalpy in Figure 5. As the binding

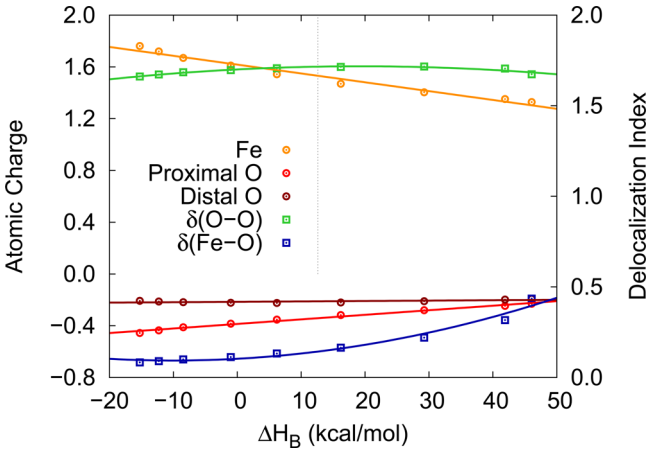

Figure 5. Atomic charges (left axis, circles) and delocalization indices (right axis, squares) for FePIm-O_2 with respect to the calculated bond-dissociation enthalpy. Results were obtained by varying range-separation parameter, ω, in the LC-BLYP functional.

energy and Fe−O delocalization index decrease, the Fe atom becomes more electropositive, while the proximal O atom becomes more electronegitive. Thus, as the degree of exact-exchange mixing is increased, the interaction becomes more ionic, with greater charge transfer from the iron to the O_2 moiety. Taken together, the atomic charges and delocalization indices illustrate that the electronic structure of the oxy-iron porphine system obtained from spin-unrestricted density-functional theory is best described by the Weiss configuration, involving antiferromagnetic coupling between the iron center and superoxide.

4. CONCLUSIONS

This article has shown that inclusion of HF exchange aids prediction of the correct ground-state multiplicity for the imidazolium-ligated iron-porphine yet destabilizes the oxygen-bound system. Of the density-functional approximations considered, only B97-D, B3LYP-D, and ωB97X-D are able to predict both the correct ground state and favorable binding of dioxygen to the iron porphine, although none are able to offer quantitative agreement with reference data for both properties. The failure of hybrid or range-separated hybrid functionals to provide an accurate Fe−O bond-dissociation enthalpy is a result of the multireference character of FePIm-O_2, the ground state of which is an open-shell singlet. None of the functionals studied, or the vast majority of available density-functional approximations,[73] are designed to describe such systems.

Analysis of the delocalization indices, computed using QTAIM, are shown to be very useful and informative tools to analyze both chemical bonding and errors in DFAs. Increasing the extent of HF exchange in a hybrid or range-separated hybrid functional is found to preferentially stabilize the high-spin state of FePIm, which is characterized by the more localized electron density, while causing the antiferromagnetic FePIm-O_2 interaction to become nonbonding. In conclusion, this work illustrates the fine balance necessary to obtain a good description of the iron porphyrin system and the significant challenge in designing appropriate density functionals to investigate systems with competing chemical effects, including charge-transfer, electron delocalization, several possible spin states, and high multireference character.

■ ASSOCIATED CONTENT

Supporting Information

Cartesian coordinates for the optimized geometries of the FePIm (triplet and quintet) and FePIm-O_2 complexes. The Supporting Information is available free of charge on the ACS Publications website at DOI: 10.1021/acs.jctc.5b00203.

■ AUTHOR INFORMATION

Corresponding Author

*E-mail: erin.johnson@dal.ca.

Notes

The authors declare no competing financial interest.

■ REFERENCES

(1) Ethirajan, M.; Chen, Y.; Joshi, P.; Pandey, R. K. *Chem. Soc. Rev.* **2011**, *40*, 340−362.
(2) Sheng, H.; et al. *Antioxid. Redox Signaling* **2014**, *20*, 2437−2464.
(3) Sun, Y.; Chen, K.; Jia, L.; Li, H. *Phys. Chem. Chem. Phys.* **2011**, *13*, 13800−13808.
(4) Ali, E.; Sanyal, B.; Oppeneer, P. M. J. *Phys. Chem. B* **2012**, *116*, 5849−5859.
(5) Tsuchida, E.; et al. *Bioconjugate Chem.* **2009**, *20*, 1419−1440.
(6) Perdew, J. P.; Zunger, A. *Phys. Rev. B* **1981**, *23*, 5048.
(7) Zhang, Y. K.; Yang, W. T. J. *Chem. Phys.* **1998**, *109*, 2604−2608.
(8) Ruzsinszky, A.; Perdew, J. P.; Csonka, G. I.; Vydrov, O. A.; Scuseria, G. E. J. *Chem. Phys.* **2006**, *125*, 194112.
(9) Mori-Sánchez, P.; Cohen, A. J.; Yang, W. J. *Chem. Phys.* **2006**, *125*, 201102.
(10) Cohen, A. J.; Mori-Sánchez, P.; Yang, W. *Science* **2008**, *321*, 792.
(11) Mori-Sánchez, P.; Cohen, A. J.; Yang, W. *Phys. Rev. Lett.* **2008**, *100*, 146401.
(12) Tozer, D. J. *J. Chem. Phys.* **2003**, *119*, 12697−12699.
(13) Dreuw, A.; Weisman, J. L.; Head-Gordon, M. J. *Chem. Phys.* **2003**, *119*, 2943−2946.
(14) Sini, G.; Sears, J. S.; Bredas, J. L. *J. Chem. Theory Comput.* **2011**, *7*, 602−609.
(15) Zheng, X.; Liu, M.; Johnson, E. R.; Contreras-Garcia, J.; Yang, W. *J. Chem. Phys.* **2012**, *137*, 214106.
(16) Steinmann, S. N.; Piemontesi, C.; Delacht, A.; Corminboeuf, C. *J. Chem. Theory Comput.* **2012**, *8*, 1629−1640.
(17) Johnson, E. R.; Salamone, M.; Bietti, M.; DiLabio, G. A. *J. Phys. Chem. A* **2013**, *117*, 947−952.
(18) Johnson, E. R.; Otero-de-la Roza, A.; Dale, S. G. *J. Chem. Phys.* **2013**, *139*, 184116.

DOI: 10.1021/acs.jctc.5b00203
J. Chem. Theory Comput. XXXX, XXX, XXX−XXX

(19) Gill, P. M. W.; Adamson, R. D.; Pople, J. A. *Mol. Phys.* **1996**, *88*, 1005−1009.
(20) Iikura, H.; Tsuneda, T.; Yanai, T.; Hirao, K. *J. Chem. Phys.* **2001**, *115*, 3540−3544.
(21) Baer, R.; Livshits, E.; Neuhauser, D. *Chem. Phys.* **2006**, *329*, 266−275.
(22) Cohen, A. J.; Mori-Sánchez, P.; Yang, W. *J. Chem. Phys.* **2007**, *126*, 191109.
(23) Vydrov, O. A.; Scuseria, G. E. *J. Chem. Phys.* **2006**, *125*, 234109.
(24) Chai, J.-D.; Head-Gordon, M. *J. Chem. Phys.* **2008**, *128*, 084106.
(25) Chai, J.-D.; Head-Gordon, M. *Phys. Chem. Chem. Phys.* **2008**, *10*, 6615−6620.
(26) Walker, V. E. J.; Castillo, N.; Matta, C. F.; Boyd, R. J. *J. Phys. Chem. A* **2010**, *114*, 10315−10319.
(27) Ugalde, J. M.; Dunietz, B. D.; Dreuw, A.; Head-Gordon, M.; Boyd, R. J. *J. Phys. Chem. A* **2004**, *108*, 4653−4657.
(28) Rovira, C.; Kunc, K.; Hutter, J.; Ballone, P.; Parrinello, M. *J. Phys. Chem. A* **1997**, *101*, 8914−8925.
(29) Sun, Y.; Hu, X.; Li, H.; Jalbout, A. F. *J. Phys. Chem. C* **2009**, *113*, 14316−14323.
(30) Liao, M.-S.; Huang, M.-J.; Watts, J. D. *J. Phys. Chem. A* **2010**, *114*, 9554−9569.
(31) Siegbahn, P. E. M.; Blomberg, M. R. A.; Chen, S.-L. *J. Chem. Theory Comput.* **2010**, *6*, 2040−2044.
(32) Radon, M.; Pierloot, K. *J. Phys. Chem. A* **2008**, *112*, 11824−11832.
(33) Vancoillie, S.; Zhao, H.; Radon, M.; Pierloot, K. *J. Chem. Theory Comput.* **2010**, *6*, 576−582.
(34) Frisch, M. J. et al. *Gaussian 09*, Revision A.1; Gaussian Inc.: Wallingford, CT, 2009.
(35) Caughey, W. S.; Barlow, C. H.; Maxwell, J. C.; Volpe, J. A.; Wallace, W. J. *Ann. N.Y. Acad. Sci.* **1975**, *244*, 1−8.
(36) Grimme, S. *J. Comput. Chem.* **2006**, *27*, 1787−1799.
(37) Becke, A. D. *Phys. Rev. A* **1988**, *38*, 3098−3100.
(38) Lee, C.; Yang, W.; Parr, R. G. *Phys. Rev. B* **1988**, *37*, 785−789.
(39) Becke, A. D. *J. Chem. Phys.* **1993**, *98*, 5648−5652.
(40) Perdew, J.; Burke, K.; Ernzerhof, M. *Phys. Rev. Lett.* **1996**, *77*, 3865−3868.
(41) Adamo, C.; Barone, V. *J. Chem. Phys.* **1999**, *110*, 6158−6170.
(42) Zhao, Y.; Truhlar, D. G. *Theor. Chem. Acc.* **2008**, *120*, 215−241.
(43) Johnson, E. R.; Becke, A. D. *Can. J. Chem.* **2009**, *87*, 1369−1373.
(44) DiLabio, G. A. *J.Phys. Chem. A* **1999**, *103*, 11414−11424.
(45) Rong, C.; et al. *Chem. Phys. Lett.* **2007**, *434*, 149−154.
(46) Bader, R. F. W.; Stephens, M. *J. Am. Chem. Soc.* **1975**, *97*, 7391−7399.
(47) Fulton, R. L. *J. Phys. Chem.* **1993**, *97*, 7516−7529.
(48) Bader, R. F. W.; Streitwieser, A.; Neuhaus, A.; Laidig, K. E.; Speers, P. *J. Am. Chem. Soc.* **1996**, *118*, 4959−4965.
(49) Fradera, X.; Austen, M. A.; Bader, R. F. W. *J. Phys. Chem. A* **1999**, *103*, 304−314.
(50) Fradera, X.; Poater, J.; Simon, S.; Duran, M.; Solà, M. *Theor. Chem. Acc.* **2002**, *108*, 214−224.
(51) Poater, J.; Solà, M.; Duran, M.; Fradera, X. *Theor. Chem. Acc.* **2002**, *107*, 362−371.
(52) Kar, T.; Ángyán, J. G.; Sannigrahi, A. B. *J. Phys. Chem. A* **2000**, *104*, 9953−9963.
(53) Chesnut, D. B.; Bartolotti, L. *J. Chem. Phys.* **2000**, *257*, 175−181.
(54) Otero-de-la Roza, A.; Johnson, E. R.; DiLabio, G. A. *J. Chem. Theory Comput.* **2014**, *10*, 5436−5447.
(55) Keith, T. A. *AIMAll* (Version 14.06.21); TK Gristmill Software: Overland Park, KS, USA, 2014. aim.tkgristmill.com (accessed June 2, 2015).
(56) Alcantara, R. E.; Xu, C.; Spiro, T. G.; Guallar, V. *Proc. Natl. Acad. Sci. U. S. A.* **2007**, *104*, 18451−18455.
(57) Scherlis, D. A.; Estrin, D. A. *Int. J. Quantum Chem.* **2002**, *87*, 158−166.
(58) Fouqueau, A.; et al. *J. Chem. Phys.* **2004**, *120*, 9473−9486.
(59) Fouqueau, A.; Casida, M. E.; Lawson Daku, L. M.; Hauser, A.; Neese, F. *J. Chem. Phys.* **2005**, *122*, 44110.
(60) Fermi, G.; Perutz, M. F.; Shaanan, B. *J. Mol. Biol.* **1984**, *175*, 159−174.
(61) Vojtěchovsk, J.; Chu, K.; Berendzen, J.; Sweet, R. M.; Schlichting, I. *Biophys. J.* **1999**, *77*, 2153−2174.
(62) Kachalova, G. S.; Popov, A. N.; Bartunik, H. D. *Science* **1999**, *284*, 473−476.
(63) Unno, M.; Chen, H.; Kusama, S.; Shaik, S.; Ikeda-Saito, M. *J. Am. Chem. Soc.* **2007**, *129*, 13394−13395.
(64) Chen, H.; Ikeda-Saito, M.; Shaik, S. *J. Am. Chem. Soc.* **2008**, *130*, 14778−14790.
(65) Olson, J. S.; Phillips, G. N. J. *J. Biol. Inorg. Chem.* **1997**, *2*, 544−552.
(66) Otero-de-la Roza, A.; Johnson, E. R. *J. Chem. Phys.* **2013**, *138*, 204109.
(67) Foster, M. E.; Wong, B. M. *J. Chem. Theory Comput.* **2012**, *8*, 2682−2687.
(68) Johnson, E. R.; Mori-Sánchez, P.; Yang, W. *J. Chem. Phys.* **2008**, *129*, 204112.
(69) Becke, A. D. *J. Chem. Phys.* **2003**, *119*, 2972−2977.
(70) Ziegler, T.; Rauk, A.; Baerends, E. J. *Theor. Chim. Acta.* **1977**, *43*, 261−271.
(71) Ess, D. H.; Johnson, E. R.; Hu, X.; Yang, W. *J. Phys. Chem. A* **2011**, *115*, 76−83.
(72) Jensen, K. P.; Roos, B. O.; Ryde, U. *J. Inorg. Biochem.* **2005**, *99*, 45−54.
(73) Becke, A. D.; Savin, A.; Stoll, H. *Theor. Chim. Acta* **1995**, *91*, 147−156.

DOI: 10.1021/acs.jctc.5b00203
J. Chem. Theory Comput. XXXX, XXX, XXX−XXX